Supplementary material: Half-life determination of ^{215}At and ^{221}Ra with high-purity radioactive ion beams

S. Bara[a,1,*], E. Jajčišinová[a,b,2,*], T. E. Cocolios[a,*], B. Andel[c], S. Antalic[c], A. Camaiani[d,e,a], C. Costache[f], K. Dockx[a], G. J. Farooq-Smith[g,a], A. Kellerbauer[b], R. Lica[f], K. M. Lynch[h], P. Marini[i], M. Piersa-Siłkowska[j,k], S. Stegemann[j,a], M. Stryjczyk[l,m,a], D. Treasa[i], P. Van Duppen[a]

[a] *KU Leuven, Instituut voor Kern- en Stralingsfysica, 3001, Leuven, Belgium*
[b] *European Commission, Joint Research Centre (JRC), Karlsruhe, Germany*
[c] *Department of Nuclear Physics and Biophysics, Comenius University in Bratislava, 84248, Bratislava, Slovakia*
[d] *Dipartimento di Fisica, Università di Firenze, I-50019, Sesto Fiorentino, Italy*
[e] *Istituto Nazionale di Fisica Nucleare, Sezione di Firenze, I-50019, Sesto Fiorentino, Italy*
[f] *Horia Hulubei National Institute for Physics and Nuclear Engineering, RO-077125, Bucharest, Romania*
[g] *Department of Oncology Physics, Edinburgh Cancer Centre, Western General Hospital, Edinburgh, United Kingdom*
[h] *School of Physics and Astronomy, The University of Manchester, M13 9PL, Manchester, United Kingdom*
[i] *University of Bordeaux, CNRS, LP2I, UMR 5797, F-33170, Gradignan, France*
[j] *CERN, CH-1211, Geneve 23, Switzerland*
[k] *Faculty of Physics, University of Warsaw, PL 02-093, Warsaw, Poland*
[l] *University of Jyvaskyla, Department of Physics, Accelerator laboratory, P.O. Box 35, FI-40014 University of Jyvaskyla, Finland*
[m] *Helsinki Institute of Physics, University of Helsinki, P.O. Box 64, FI-00014 Helsinki, Finland*

Abstract

We report on the systematic investigations in the study of the half-life of ^{215}At and ^{221}Ra with the CRIS decay spectroscopy station (DSS) and the alpha setup (ASET) at CERN-ISOLDE. In particular, we explore systematic effects on the α-decay energy spectra and the fit conditions for the half-life.

1. IS471

The data from the CRIS campaign were collected in November 2014. ^{219}Fr was used as a reference beam to assess the performance of the experimental setup because of its well known α decay and the short half-life of its progeny that ensured minimal contamination of the setup. The total spectra collected on either detectors are shown in Fig. 1.

Coincidences were created by searching for any event in either detector for 10 ms following an event and recording those as pairs. As soon as a second event is identified, the search is ended and a new search is started from the next event onward. The time behavior of the coincidences is then built by requiring energy gates corresponding to the α decay of either ^{219}Fr or ^{215}At, in that order. A random coincidence time spectrum is generated by imposing the reversed order, and is subtracted from the coincident spectrum. When the random coincidences histogram is subtracted from the real coincidences one, the fitting routine automatically propagates the uncertainties to the final histogram. The time behavior of the coincidence for the full-full, full-annular, and annular-full configurations are shown in Fig. 2. The residuals were calculated as a difference between the data and the fit, and divided by the uncertainty of the data.

Systematic effects were investigated on the stability of the fit of these half-life curves according to Eq. 1 of the main article. Given the limited statistics from this data set, all fits were performed with maximum likelihood. Given the applied background subtraction, Eq. 1 was applied with $c = 0$.

*Corresponding author
[1] silvia.bara@kuleuven.be
[2] erika.jajcisinova@student.kuleuven.be

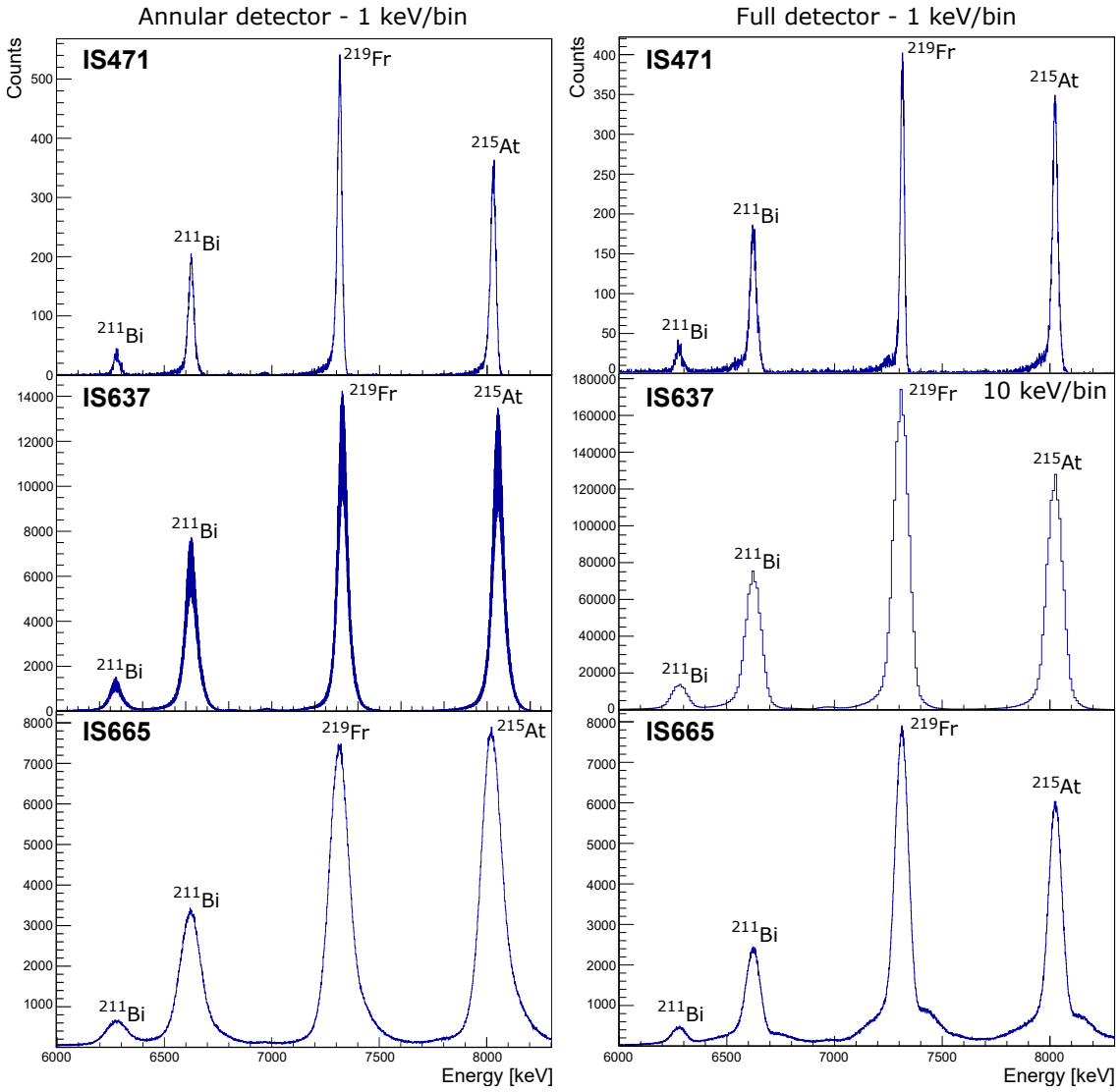

Figure 1: Alpha-decay energy spectra of ^{219}Fr from the annular (left) and full (right) detector, during the IS471 campaign (top), IS637 campaign (middle), and IS665 campaign (bottom). The bin size is 1 keV.

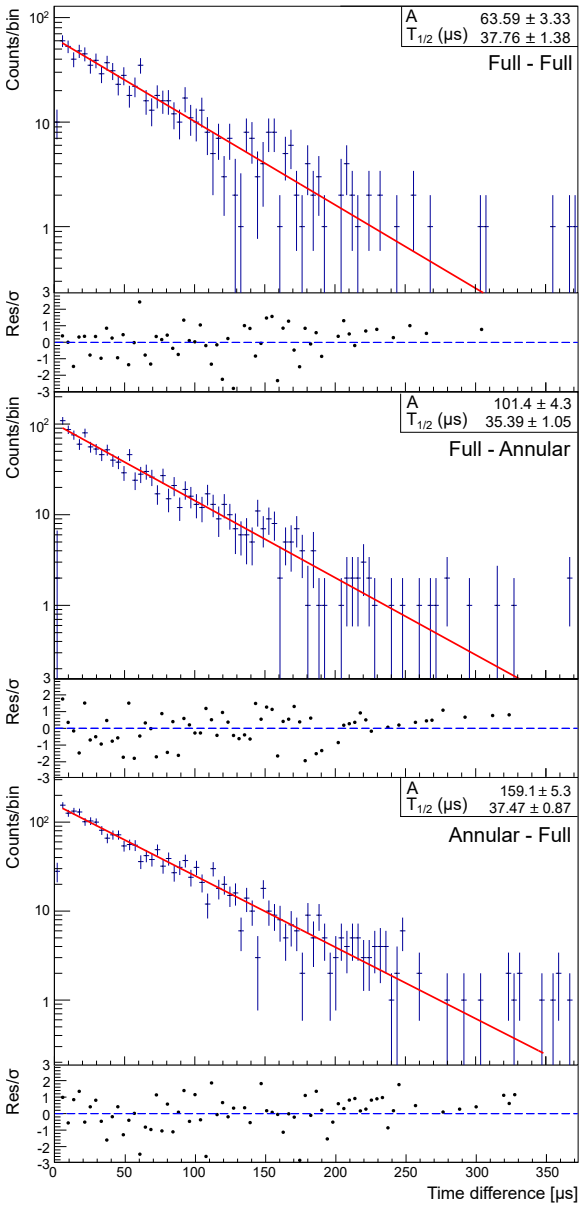

Figure 2: **IS471** - Decay curve of ^{215}At from the IS471 data for the full-full (top), full-annular (middle) and annular-full (bottom) coincidence configurations. The red line corresponds to the best fit of the half-life once all systematic effects are accounted for. The insets provide the output of the fit. The bin size is 4 μs and the residuals for each plot are provided. The residuals correspond to difference between data and fit, divided by uncertainty of data.

Several parameters were investigated to see their effect on the half-life fit results. The range for the fit was considered by changing either the starting time or end time of the fit, to see to which value the fit converged and provided the best uncertainty once converged. The data are presented in Fig. 3. It is concluded that the best fitting range is from 4 μs to 350 μs, which corresponds nearly to 10 half-lives.

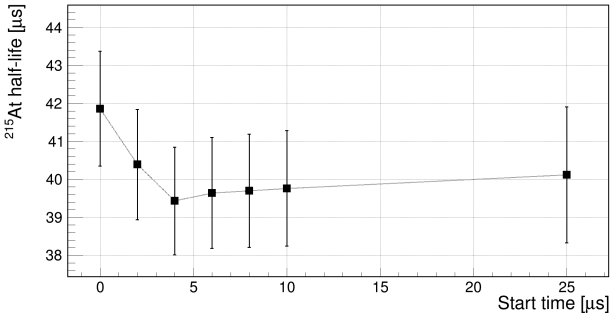

(a)

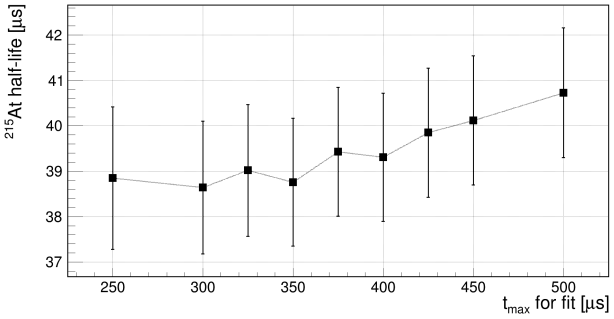

(b)

Figure 3: **IS471** - Systematic effect of changing a) the start of the fitting range or b) the end of the fitting range on the half-life value. The best parameters are found when the half-life result starts stabilizing around a certain value and has the smallest uncertainty, namely with a range from 4 μs to 350 μs.

The next parameter investigated is the binning of the half-life histogram. Bin sizes ranging from 0.5 μs to 5 μs were considered. For the highest value, the fit was started at 5 μs to discard the first bin altogether. The results are shown in Fig. 4 and show that the best bin size is 4 μs. This high value compared to the other data sets is due to the low statistics of these data.

The last parameter investigated is the width of the energy windows around each α-decay energy peaks. For consistency, the windows were evaluated in units of σ of a Gaussian fit on the α-decay line. Ranges from 1 to 10 σ have been considered. The resulting half-lives are shown in Fig. 5, from which it is concluded that the largest energy window is most appropriate for this data set.

Those parameters were then applied to generate the three fits presented in Fig. 2 and reported in Table 1 of the main text.

These systematic studies were used to determine a general systematic uncertainty. For each parameter analysed, a reasonable range was chosen and the spread of the half-life within this range was taken as systematic uncertainty coming from that specific parameter. Systematic uncertainties from parameters that could be correlated between each other, like t_{start} and t_{max}, were added linearly, and the result in quadrature to the rest. The details can be found in Table 1, and the final systematic uncertainty resulted in 0.9 μs.

2. IS637

The data from the IS637 experiment presented in this paper were collected in July 2018. The beam of mass A=219 was delivered to the ASET experimental setup for the studies of ^{219}Fr as part of the systematic

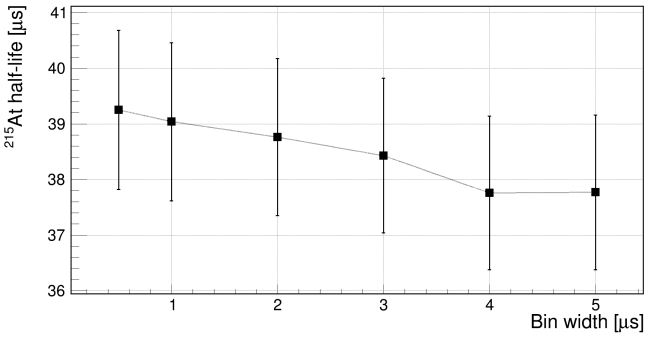

Figure 4: **IS471** - Systematic effect of changing the bin size on the half-life value. The best parameter is found when the half-life result starts stabilizing around a certain value and has the smallest uncertainty, namely with a bin size of 4 μs.

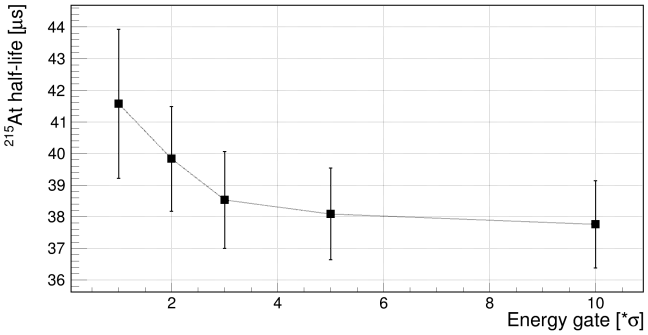

Figure 5: **IS471** - Systematic effect of changing the energy gate on the α lines on the half-life value. The best parameters are found when the half-life result starts stabilizing around a certain value and has the smallest uncertainty, namely with an energy window of 10 σ around each peak.

Table 1: **IS471**: Details on the systematic uncertainty estimation for the IS471 campaign. For each parameter investigated, the range used to obtain the uncertainty is given. t_{start} and t_{max} are added linearly, since they are correlated. The result is then added in quadrature to the other values.

Parameter	**Range**	**Systematic uncertainty [μs]**
t_{start} [μs]	4 - 25	0.25
t_{max} [μs]	250 - 400	0.31
Bin width [μs]	0.5 - 5	0.63
Energy gate [σ]	3 - 10	0.39

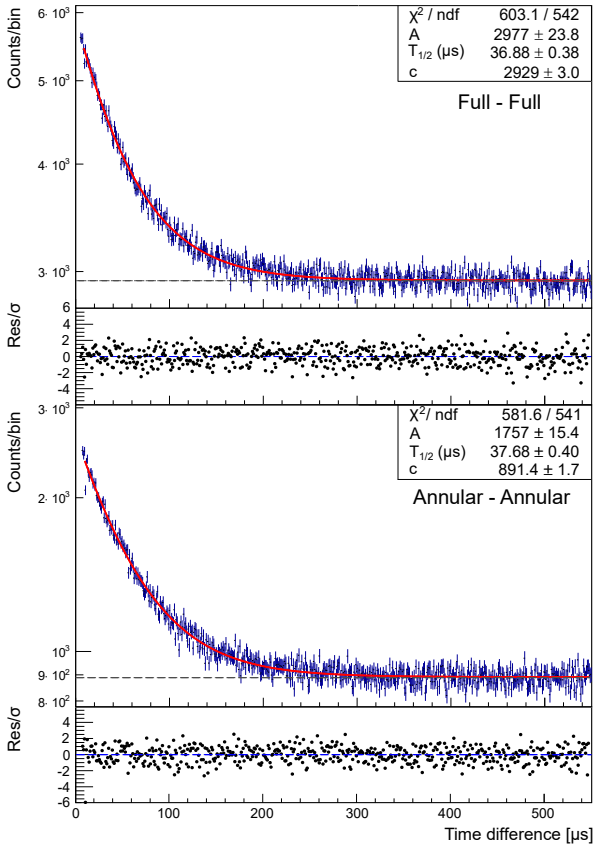

Figure 6: **IS637** - Decay curve of ^{215}At from the IS637 data for the full-full (top) and annular-annular (bottom) configurations within coincidence window of 555 μs. The fitting range is for full-full (6-550 μs) and annular-annular (7-550 μs) The red line corresponds to the best fit of the half-life once all systematic effects are accounted for. The insets provide the output of the fit. The first data-points are still influenced by the dead time. The bin size is 1 μs and the residuals for each plot are provided. Grey dashed lines represent constant background. The residuals correspond to difference between data and fit, divided by uncertainty of data.

study of Fr, Ra and Ac beam characterization.

Due to the non-synchronization of the data acquisition modules, the coincidences were performed only within the same detector. The coincidence code was based on comparing the delay time between two events that occurred within a coincidence window of 555 μs, corresponding to fifteen times the expected half-life of ^{215}At of 37 μs. If the consecutive events occurred within a time bigger than our coincidence window, the time is moved one step forward. In order to get a time behavior of coincidence of our interest the energy gates had to be set to the ^{219}Fr and ^{215}At α-particle energies. As the coincidences were performed within the same detector, an analysis of the dead time was performed which resulted in a dead time of 6 μs during which the electronic module did not accept any event. The time behavior of the coincidences for the full-full and annular-annular configurations are shown in Fig. 6.

During the analysis several parameters were investigated to establish their influence on the half-life determination. The first one is the fitting range that was changed from the start of the fit (0-12 μs) and from its end (300-450 μs). As showed in Fig. 7 when the fit was started too early (relating to the dead time) the half-life value had a high offset, while, on the other hand, prolonging the end time for fit showed to provide stabilizing effect.

The second investigated effect is the impact of the bin width used to obtain the decay curves. The bin size varied from 0.37-3.7 μs and the energy gate was set to 6-7 σ and curve fitted from maximum point to

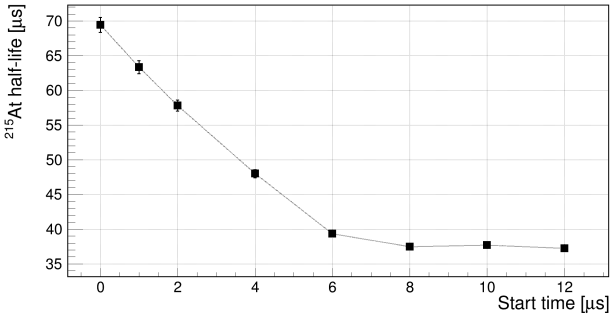

(a)

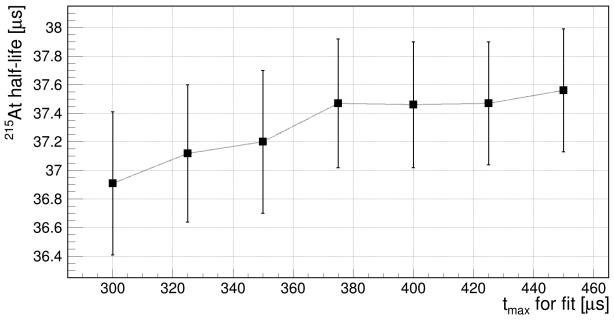

(b)

Figure 7: **IS637** - Systematic effect of changing a) the start of the fitting range (end time 375 μs) or b) the end of the fitting range on the half-life value (start time 8 μs). The best parameters are found when the half-life result starts stabilizing around a certain value and has the smallest uncertainty, namely with a range from 8 μs to 370 μs.

the end of the range. Theoretically, the fit value should not depend on the bin size and with our analysis we proved that the half-life values are consistent with each other within their errors (see Fig. 8).

The last investigated effect is the size of energy gates used to select only the coincidences coming from the decay of ^{219}Fr into ^{215}At. The energy gate size varied from 3-16 σ. From this point of view, the use of excessively narrow or wide energy gates could reduce the accuracy of the extracted half-life however if one chooses energy gate between 10-16 σ it would results in the same level of uncertainty (see Fig. 9).

The best obtained parameters were then applied to generate the two fits presented in Fig. 6 and in Table 1 of the main text with the fitting range for full-full 6-550 μs and annular-annular 7-550 μs binned as 1 bin per μs with wide energy gates 13-15 σ.

Similarly to what was done for the IS471 data, a systematic uncertainty was determined from the scatter of the half-life coming from each fitting parameter. The details can be found in Table 2, and the final systematic uncertainty resulted in 0.6 μs.

3. IS665

The data presented in this section were collected in August 2021 as side measurements of the IS665 experimental campaign. A beam of ^{219}Fr was implanted in the ASET experimental setup to study the half-life of its daughter ^{215}At. A RaF^+ molecular beam of mass $A = 221+19 = 240$ was later implanted to study the half-life of ^{221}Ra. The total spectra collected with both the annular and the full detectors are shown in Fig. 1 for ^{219}Fr and in Fig. 10 for ^{221}Ra.

3.1. ^{215}At

Coincidences were created between the two silicon detectors with procedures similar to those described both in Section 1 for coincidences between different detectors, and in Section 2 for coincidences within the

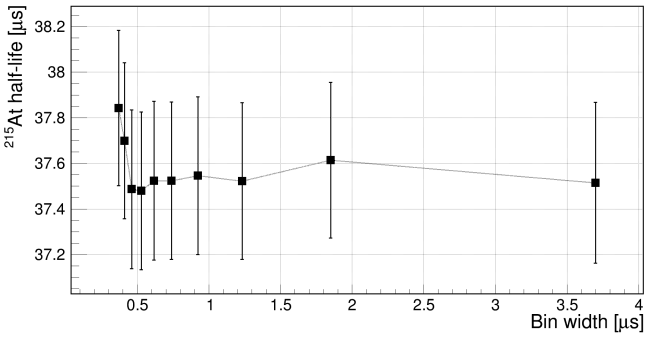

Figure 8: **IS637** - Systematic effect of changing the bin size on the half-life value. The best parameter is found when the half-life result starts stabilizing around a certain value and has the smallest uncertainty, namely with a bin size around 1 μs.

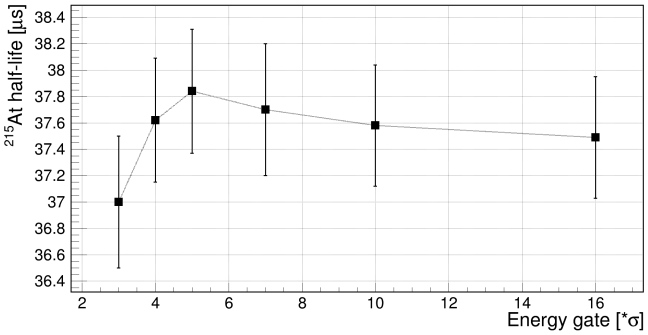

Figure 9: **IS637** - Systematic effect of changing the energy gate on the α lines on the half-life value. The best parameters are found when the half-life result starts stabilizing around a certain value and has the smallest uncertainty, namely with an energy window between 10 to 16 σ around each peak.

Table 2: **IS637**: Details on the systematic uncertainty estimation for the IS637 campaign. For each parameter investigated, the range used to obtain the uncertainty is given. t_{start} and t_{max} are added linearly between them, since they are correlated. The result is then added in quadrature to the other values.

Parameter	**Range**	**Systematic uncertainty [μs]**
t_{start} [μs]	8 - 12	0.22
t_{max} [μs]	300 - 450	0.24
Bin width [μs]	0.37 - 3.7	0.12
Energy gate [σ]	3 - 16	0.29

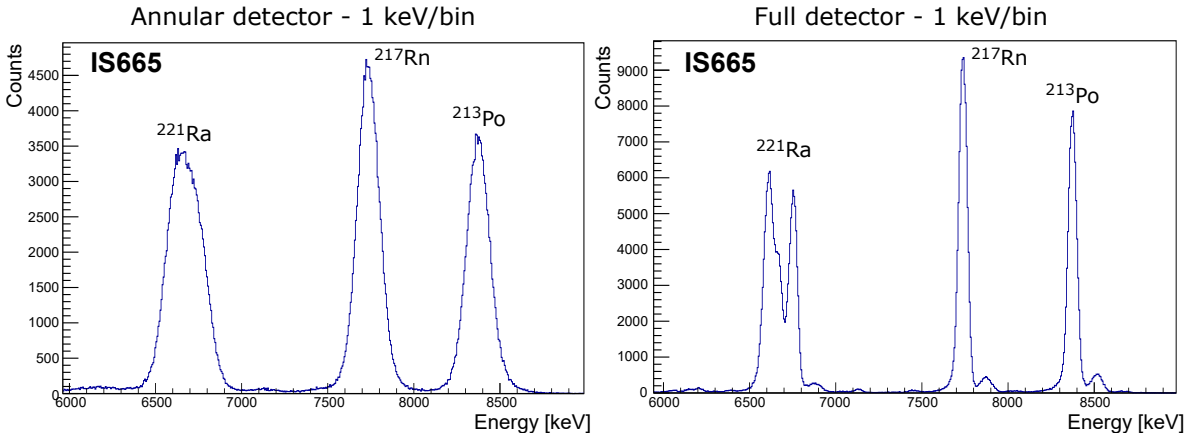

Figure 10: **IS665** - Alpha-decay energy spectra of ^{221}Ra during the IS665 campaign for the annular (left) and full (right) detector.

same detector. The coincidence window used in this case was about 555 μs. Energy gates on the α line of ^{219}Fr and ^{215}At were used to create the decay curves from which to obtain the ^{215}At half-life.

Different coincidence configurations were possible and the results are shown in Fig. 12. A misplacement of the ladder inside ASET made it not possible to study the 'full - full' configuration due to extremely low coincidences statistics.

From the annular-annular configuration the dead-time of the system was estimated to be 8 μs this being the minimum time the system needs to process two consecutive events. However, that configuration suffered globally from very high rates that resulted in many pile-up and baseline saturation events that affected the acquisition in that same timescale, preventing the use of this configuration for the final analysis. Therefore, only opposite detectors are considered for this campaign.

This observation triggered a more thorough analysis of the time behavior of single events in the data stream, from which it was concluded that the instantaneous data rate was highly correlated with the proton irradiation of the target. The PS Booster delivers short proton pulses of a few 100 ns width, separated with a multiple of 1.2 s. The directly produced ^{219}Fr is then released within 700 ms in a high rate, while a continuous, lower rate of ^{219}Fr is supplied from ^{223}Ac decaying within the target matrix. This resulted in two different conditions for the data acquisition, with the high-rate data facing substantial time distortions due to dead time, pile up, and baseline saturation. All data collected within the first 700 ms after a proton pulse were thus discarded, resulting in a reduction of the total statistics by 40-50 %. Fig. 11 shows the proton pulses structure and the selected regions. Moreover, some events were found to be wrongly unflagged as pile-up: these were consecutive events presenting the same energy and time difference too short with respect to the trapezoid filter time window. They should have been recognized as pile-up by the software and assigned null energy, but a bug in the software made it so that some of those events were not recognized properly. Therefore, it was decided to manually remove them in post-analysis without, however, influencing too much the results as their contribution to the total statistics is about 1 %.

The obtained half-life spectra are presented in Fig. 12.

In the whole procedure there were different factors that needed to be set and that can influence the outcome of the fit. Therefore, systematic effects of these parameters were investigated by changing one of them at a time in one of the configuration studied (annular - full). First, the fitted time range was studied by changing both the value of the start time and the end time of the fit while leaving the other one fixed. The best parameters were selected as those that made the fit converging while providing the smallest uncertainty. The results are shown in Fig. 13. From the thorough analysis performed on the data, we noticed when looking at random coincidences (taking, for example, ^{215}At as start and ^{219}Fr as stop) that their trend was not constant, and it was lower at small time differences. A similar behaviour can be seen in

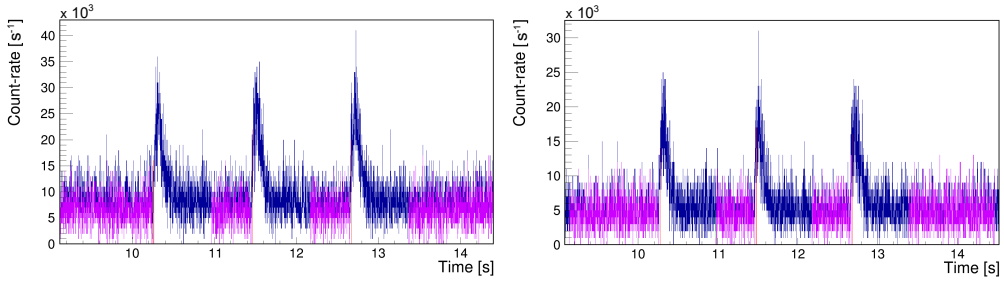

(a) (b)

Figure 11: **IS665** - Timestamp zoom of the annular (left) and full (right) detectors during implantation of ^{219}Fr, showing the proton pulses structure and the higher rate corresponding to each one of them. The blue plot represents the total statistics, while the purple shows the regions selected for the analysis.

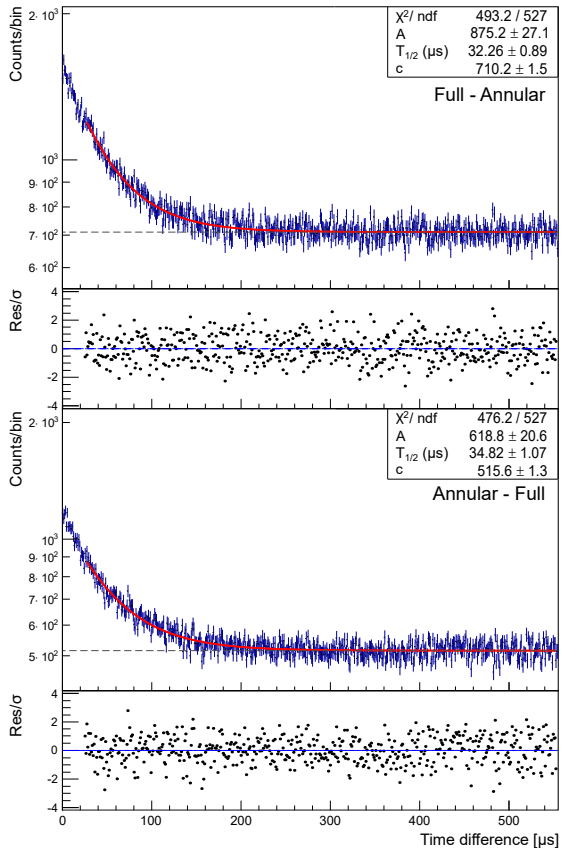

Figure 12: **IS665** - Decay curve of ^{215}At for the full-annular (top) and annular-full (bottom) configurations. The red line corresponds to the best fit of the half-life once all systematic effects are accounted for. The insets provide the output of the fit. The first data-points are still influenced by the dead time. The bin size is 1 μs and the residuals for each plot are provided. Grey dashed lines represent constant background. The residuals correspond to difference between data and fit, divided by uncertainty of data.

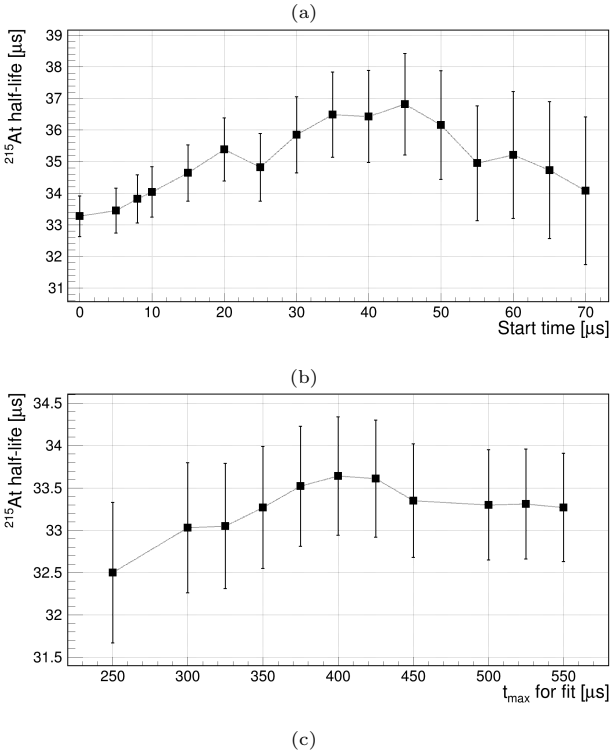

Figure 13: **IS665** - Systematic effect of changing a) the start of the fitting range or b) the end of the fitting range on the half-life value in annular - full configuration. In a) t_{max} was kept to 555 μs, while in b) t_{start} was kept at 0 μs. The chosen parameters are 25 μs as start of the fit and 555 μs as t_{max}.

fig. 13a). For this reason, it was decided to avoid the initial range, and start the fit from 25 μs.

The second parameter investigated is the bin width of the decay curve histogram. Different sizes were tested and Fig. 14 shows that this parameter does not have a significant influence on the fitted half-life. A bin width on 1 μs is chosen for the rest of the fits.

Finally, the effect on the fitted half-life of the energy gates width used on ^{219}Fr and ^{215}At to create the decay curves is investigated. In this case the effect is more visible and the chosen energy gate is the one corresponding to 6 σ. The smaller range in units of σ compared to the other two campaigns arises from the lower resolution achieved in that experiment, and the actual energy range is comparable.

The same procedure used for the other two experimental campaigns was used to determine the systematic uncertainty. The details can be found in Table 3, and the final systematic uncertainty resulted in 0.9 μs.

3.2. ^{221}Ra

Similarly to the tests just described for ^{215}At, several key parameters were explored for ^{221}Ra. In this case, the decay curves were obtained by gating on the α lines and looking at their time evolution. Because the daughter and grand-daughter of ^{221}Ra are in secular equilibrium with the mother, the ^{221}Ra half-life can be extracted by gating on any of these observed α transitions. Figure 16 and 17 show the results obtained from different energy gates for both annular and full detector. From the annular-annular coincidence configuration of the ^{215}At data a dead-time of 8 μs due to the shaping parameters of the trapezoidal algorithm used for the Pulse Height Analysis of the acquisition system was determined. The dead-time correction was performed on the ^{221}Ra data using the equation 1

$$n = \frac{m}{1 - m \cdot \tau} \tag{1}$$

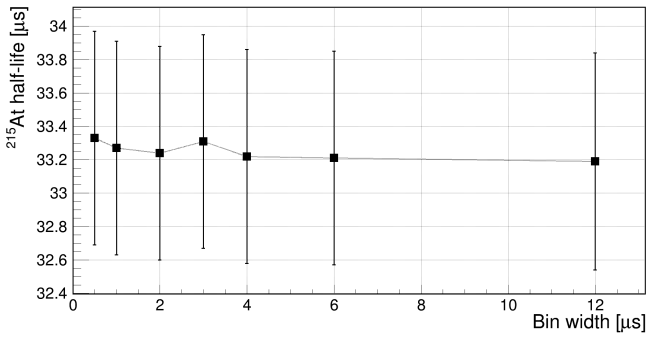

Figure 14: **IS665** - Systematic effect of changing the bin size on the half-life value in annular - full configuration. The best parameter is found when the half-life result starts stabilizing around a certain value and has the smallest uncertainty. No significant influence of this parameter is observed, so a bin size of 1 μs is chosen.

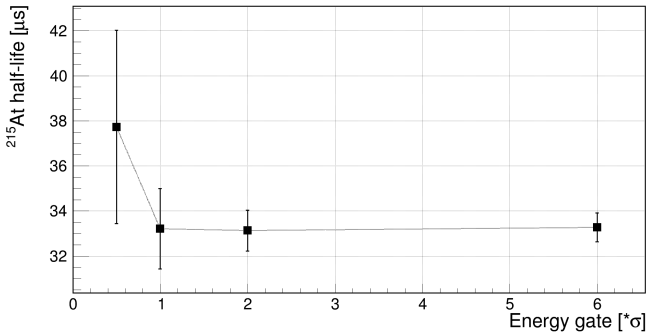

Figure 15: **IS665** - Systematic effect of changing the energy gate on the α lines on the half-life value in annular - full configuration. The best parameters are found when the half-life result starts stabilizing around a certain value and has the smallest uncertainty, namely with an energy window of 6 σ around each peak.

Table 3: **IS665**: Details on the systematic uncertainty estimation for the IS637 campaign. For each parameter investigated, the range used to obtain the uncertainty is given. t_{start} and t_{max} are added linearly between them, since they are correlated. The result is then added in quadrature to the other values.

Parameter	**Range**	**Systematic uncertainty** [μs]
t_{start} [μs]	25 - 80	0.76
t_{max} [μs]	350 - 550	0.15
Bin width [μs]	0.1 - 2	0.05
Energy gate [σ]	1 - 6	0.06

reported in Chapter 4 of Knoll (2010) for the non-paralyzable model, where n represents the true rate, m the measured rate and τ the system dead-time for which the value of 8 μs was used in this case. Potential contamination from ^{222}Ra ($T_{1/2}$ = 38.0(5) s from Studier and Hyde (1948)) in the beam was investigated and estimated to be below 1%. Such contamination does not affect the extracted half-life of ^{221}Ra beyond the systematic uncertainty. The structures observed in the residuals plots from 400 s onwards are due to an effect of the number of bins used to create the decay curve. The implementation of a more refined binning was, however, necessary to determine the half-life with the smallest uncertainty from the main part of the curve.

First of all, the effect of two different fitting methods were studied. For low statistics cases the maximum likelihood provides a better fit than the least squared method. This is evident from Fig. 18, where the values fitted from the different α gates agree well within error bars when using the maximum likelihood method, while they diverge more when using the least squares method. For this reason, it was decided to use the maximum likelihood method.

The first parameter investigated for ^{221}Ra data is the time range used for the fit. In this case, the decay part came after an implantation, so the time at which the implantation stopped and the decay started might influence the result of the fit. Since we did not have an exact time at which the implantation stopped, in order to investigate the effect of this parameter eq. 1 was re-written in order to make the dependence on the implantation time explicit. The equation used is

$$y = A \cdot \left(e^{\frac{ln(2)\cdot t_{impl}}{T_{1/2}}} - 1 \right) \cdot e^{-\frac{ln(2)\cdot t}{T_{1/2}}} + c, \tag{2}$$

In this equation, A represents the implantation rate and $T_{1/2}$ the half-life of ^{221}Ra, and are fitted from the curve, while t_{impl} is the implantation time. Finally, c is a fitted constant to account for the background. The production rate is approximated as a constant. Fig. 19 show the results of the ranges studied. The implantation time chosen is 170 s.

Second, the bin width of the decay curve is studied. Fig. 20 shows that the bin size does not have a big impact. The optimal width is found to be 1 s.

Then, the width of the energy gates used to create the decay curves was investigated. In this case, only the single line gates are shown in Fig. 21. The best gate width is chosen to be 7 σ for the annular and 11 σ for the full detector.

The same procedure used for the ^{215}At case was used to determine the systematic uncertainty for ^{221}Ra as well. The details can be found in Table 4. The systematic uncertainty from the annular detector resulted in: 0.55 s for the ^{221}Ra gate, 0.57 s for the ^{217}Rn, and 0.49 s for the ^{213}Po. From the full detector the different values were: 0.50 s for the ^{221}Ra gate, 0.70 s for the ^{217}Rn, and 0.55 s for the ^{213}Po. Therefore, as systematic uncertainty it was decided to take the average of the three values found in each case, resulting in 0.5 s for the annular detector and 0.6 s for the full. The two detectors present similar systematic uncertainties, and for the final value it was decided to take the more conservative one of 0.6 s.

References

G. F. Knoll, Radiation Detection and Measurement, Wiley, 2010.

M. H. Studier, E. K. Hyde, A new radioactive series—the protactinium series, Phys. Rev. 74 (1948) 591–600. URL: https://link.aps.org/doi/10.1103/PhysRev.74.591. doi:10.1103/PhysRev.74.591.

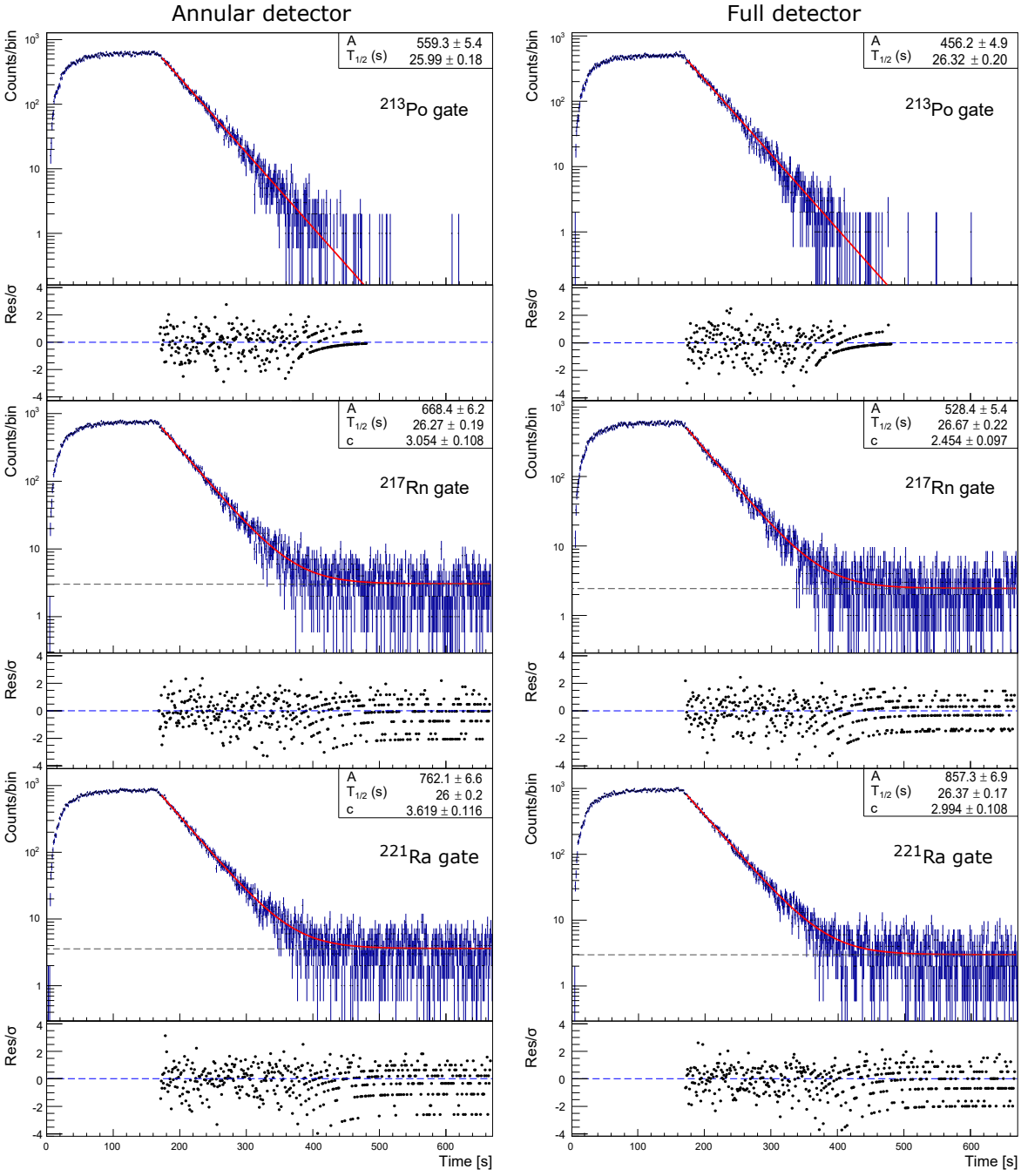

Figure 16: **IS665** - Decay curves of ^{221}Ra from the IS665 data from the annular (left) and full (right) detectors and the different energy gates studied. The red line corresponds to the best fit of the half-life once all systematic effects are accounted for. The insets provide the output of the fit. The bin size is 1 s and the residuals for each plot are provided. Grey dashed lines represent constant background. For the ^{213}Po α gate the parameter c was fixed to 0, as the curve doesn't show any background. The residuals correspond to difference between data and fit, divided by uncertainty of data. The structures in the residuals plot that can be observed from 400 s onwards are an effect due to the choice of the bin size on discrete number of counts.

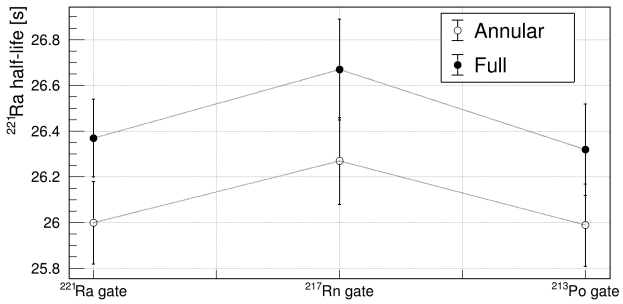

Figure 17: **IS665** - Overview of the results obtained for the ^{221}Ra half-life obtained from the different energy gates.

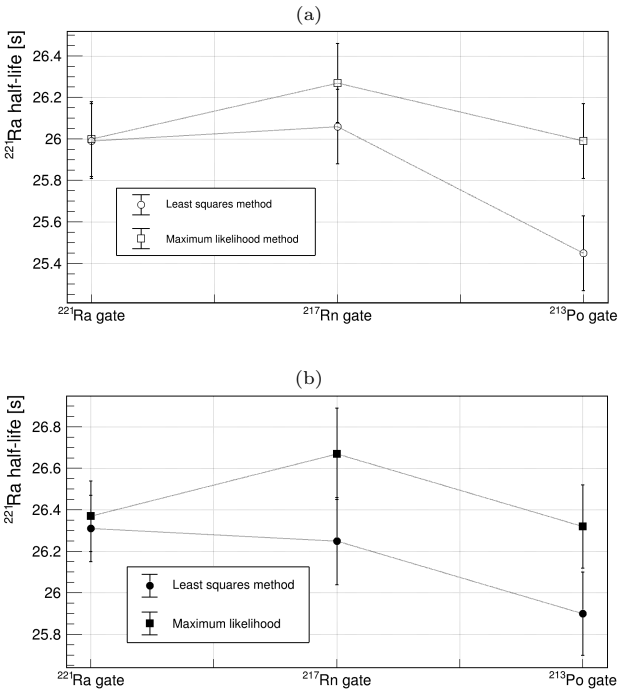

Figure 18: **IS665** - Systematic effect of changing the fitting method on the half-life value studied in a) annular and b) full detector. The different α gates investigated are shown.

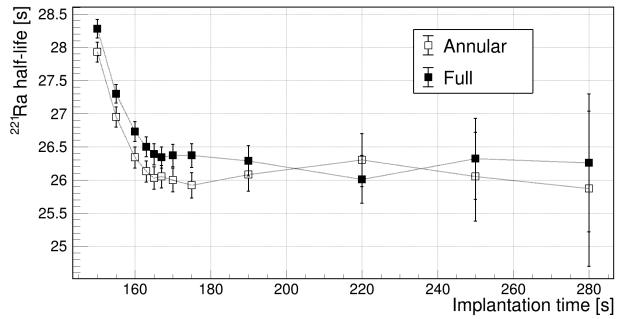

Figure 19: **IS665** - Systematic effect of changing the implantation time on the half-life value studied in annular and full detector for the ^{221}Ra α gate. The implantation time chosen is 170 s, where we are sure that the beam was stopped.

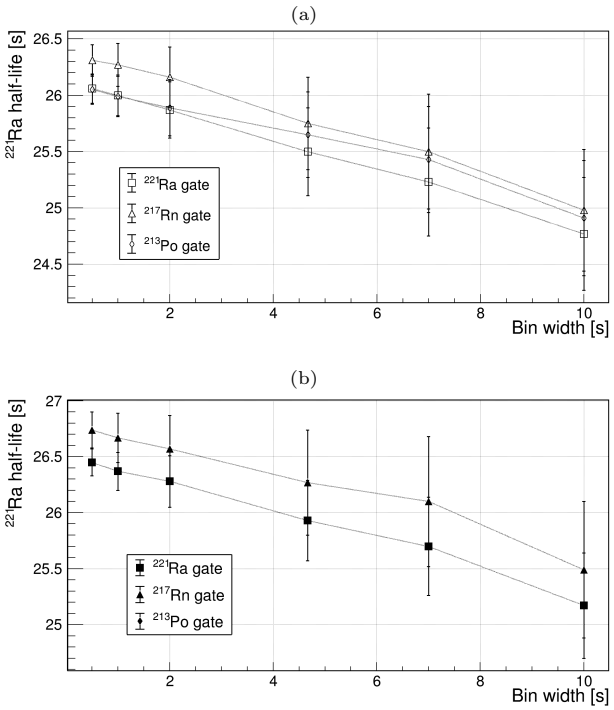

Figure 20: **IS665** - Systematic effect of changing the bin size on the half-life value studied in a) annular and b) full detector. The different α gates investigated are shown. The best parameter is found when the half-life result starts stabilizing around a certain value and has the smallest uncertainty, namely with a bin size of 1 s.

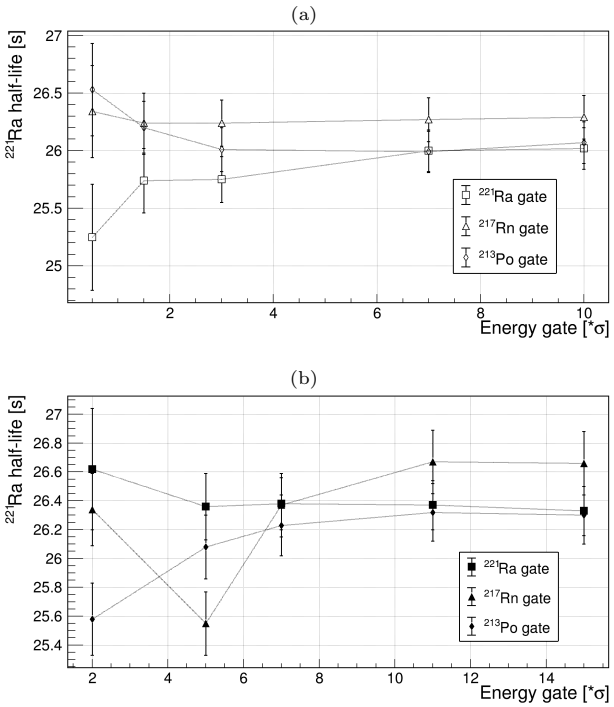

Figure 21: **IS665** - Systematic effect of changing the energy gate on the α lines on the half-life value studied in a) annular and b) full detector. The different α gates investigated are shown. The best parameters are found when the half-life result starts stabilizing around a certain value and has the smallest uncertainty, namely with an energy window of 7 σ and 11 σ around each peak for the annular and the full detector, respectively.

Table 4: **IS665**: Details on the systematic uncertainty estimation for the IS637 campaign. For each parameter investigated, the range used to obtain the uncertainty is given. t_{start} and t_{max} are added linearly between them, since they are correlated. The result is then added in quadrature to the other values.

Detector	**^{221}Ra**	**^{217}Rn**	**^{213}Po**
	Syst. Uncert. [s]	Syst. Uncert. [s]	Syst. Uncert. [s]
Annular	0.13	0.30	0.22
Full	0.18	0.38	0.25

(a) t_{impl} in the range (160 - 250) s

Detector	**^{221}Ra**	**^{217}Rn**	**^{213}Po**
	Syst. Uncert. [s]	Syst. Uncert. [s]	Syst. Uncert. [s]
Annular	0.46	0.48	0.39
Full	0.45	0.43	0.41

(b) Bin width in the range (0.5 - 10) s

Detector	**^{221}Ra**	**^{217}Rn**	**^{213}Po**
	Syst. Uncert. [s]	Syst. Uncert. [s]	Syst. Uncert. [s]
Annular	0.28	0.04	0.20
Full	0.11	0.40	0.08

(c) Energy gate in the (0.5 - 10)·σ range for the annular detector and in the (2 - 15)·σ range for the full.